Research Article

Dominik Kukla*, Adam Kondej, Sylwester Jończyk, Piotr Lasota, Jakub Tabin, Daniela Schob, Robert Roszak, Jakub Kawałko, Andrzej Zagórski, and Mateusz Kopec

Eddy current methodology in the non-direct measurement of martensite during plastic deformation of SS316L

https://doi.org/10.1515/eng-2025-0118
received October 11, 2024; accepted April 27, 2025

Abstract: This study examines the use of various eddy current induction techniques to evaluate the stability of austenite in SS316L steel subjected to plastic deformation. This deformation, which occurs locally in austenitic steel structures under operational loads, leads to a martensitic transformation. This transformation affects both the mechanical and magnetic properties of the steel. The martensitic phase content, being ferromagnetic, can be quantitatively assessed using a ferritoscope and other magnetic induction methods. The research explores techniques based on the analysis of impedance signal changes obtained using the NORTEC defetoscope and the WIROTEST device developed by the author's team. By examining the phase angle, ET signal amplitude, and resonance frequency changes in the eddy current excitation system, the study aims to quantitatively assess the martensitic phase content in samples subjected to plastic deformation. These results were verified through comparison with data from a ferritoscope and X-ray diffraction analysis. Additionally, the eddy current technique facilitates surface screening of the specimen, making it possible to identify cracks and locate the martensitic transformation front in areas of stress concentration.

Keywords: eddy current, martensitic transformation, additive manufacturing, stainless steel, non-destructive testing, WIROTEST device

*** Corresponding author: Dominik Kukla**, Łukasiewicz Research Network, Warsaw Institute of Technology, Warsaw, Poland; Institute of Fundamental Technological Research Polish Academy of Science, Warsaw, Poland, e-mail: dkukla@ippt.pan.pl
Adam Kondej, **Sylwester Jończyk**, **Piotr Lasota:** Łukasiewicz Research Network, Warsaw Institute of Technology, Warsaw, Poland
Jakub Tabin, **Mateusz Kopec:** Institute of Fundamental Technological Research Polish Academy of Science, Warsaw, Poland
Daniela Schob: Brandenburg University of Technology Cottbus-Senftenberg, Senftenberg, Germany
Robert Roszak: Chair of Engineering Mechanics and Machine Dynamics, Brandenburg University of Technology Cottbus-Senftenberg, Senftenberg, Germany; Faculty of Mechanical Engineering, Poznan University of Technology, Poznań, Poland
Jakub Kawałko: Academic Centre for Materials and Nanotechnology, AGH University of Science and Technology, Krakow, Poland
Andrzej Zagórski: Faculty of Materials Science, Warsaw University of Technology, Warsaw, Poland

1 Introduction

Austenitic steels are widely used in various industrial applications due to their high mechanical strength, corrosion resistance, and the stability of their non-magnetic properties, particularly in electrical and energy sectors. In these applications, maintaining the stability of paramagnetic austenite is crucial, as the formation of a ferromagnetic martensitic phase can occur under operational loads, both mechanical and thermal. The stability of austenite is primarily influenced by its chemical composition and the content of stabilizing alloying elements.

Austenitic steels are susceptible to martensitic transformation under plastic deformation conditions [1], and this process is more intensive at low temperatures [2]. It has been reported that in the case of 304 steel, ε-martensite (hexagonal close-packed [HCP], paramagnetic) forms at the beginning of deformation and reaches a peak value at about 5% of tensile strain. After exceeding this value, the volume fraction of this phase decreases to almost zero at 20% of plastic strain. On the other hand, the volume fraction of α'-martensite (body-centered cubic [BCC], ferromagnetic) increased steadily with deformation. At higher strain values, the α' phase was the only martensite phase present in the material volume [3]. The transformation is accompanied by a change in the magnetic properties of the steel, which allows the use of magnetic techniques to assess its effects [4].

Similar results were reported for the AISI 316 steel deformed during rolling and subsequent tension test [5]. These properties are of great importance in the case of

parts manufactured using additive technologies, because during the printing process, ferrite is precipitated at the grain boundaries of austenitic steel, the share of which reaches 6% [6,7]. Since the ferrite volume fraction in the structure of austenitic steel can adversely affect fatigue strength [8,9] it is advisable to control its content. The formation of martensite can be detected and evaluated by X-ray diffraction (XRD) [10] neuron diffraction [11], electron backscatter diffraction (EBSD) [12], magnetic methods including the eddy current method [13], metallography, and other techniques [14]. Monitoring the ferrite content released during martensitic transformation is crucial for evaluating the corrosion resistance of steel. Corrosion studies have demonstrated that martensitic transformation, induced by cold forming processes and cyclic loading conditions, significantly affects the corrosion resistance of AISI 316 austenitic stainless steel [15,16]. The formation of martensite is highly dependent on factors such as chemical composition, austenitic grain size [17], deformation temperature [18], and other variables. One should highlight that eddy current method is particularly sensitive to changes in the electrical resistivity and magnetic permeability of materials, which are influenced by variations in chemical composition, hardness, mechanical strength, and the degree of cold work. Consequently, this technique provides an indirect measurement of the overall physical and chemical properties of a material. It has been shown to be sensitive enough to detect phase transformations in stainless steels [19].

Plastic deformation of conventional and additive manufacture (AM) specimens may significantly influence their magnetic properties due to deformation-induced martensitic transformation [20]. The metastable ASSs exhibit tendency toward diffusion-free phase transformation during plastic deformation, especially when temperatures tend to 0 K [21]. In this process, initial austenite with a face-centered cubic (γ) structure transforms into martensite ε with a HCP structure and subsequently into martensite α' with a BCC structure. It is worth noting that the transformation can also occur directly and, during tension at room temperature, mainly martensite α' is observed [21,22].

Therefore, this article presents an investigation into the stability of austenite in 316 steel samples, produced from both rolled sheets and *via* AM, under static tensile loading conditions.

2 Methodology

The tests were conducted on two types of flat specimens: conventional (R) 316L and AM 316L.

The conventional specimens were fabricated using electrical discharge machining from a commercial 316L stainless steel sheet (2 mm thickness) with the tensile axis parallel to the rolling direction (RD). The semi-products were supplied in cold-rolled and annealed conditions (Figure 1). In such a form, the materials are typically used for structural components working in cryogenic conditions, down to the temperature of superfluid helium, 1.9.

The AM process utilizes Ultrafuse 316L, a metal–polymer composite filament specifically engineered for fused filament fabrication (FFF). This filament comprises over 80% metal powder, bound by a unique polymer matrix that is fully removed during debinding and sintering. The result is a high-strength, corrosion-resistant part composed entirely of 316L stainless steel. The printing process was conducted using an Ultimaker S5 printer with the following optimized parameters: a glass print platform coated with Magigoo PRO metal adhesive, a 0.4 mm hardened steel nozzle, platform temperature of 110°C, and printing temperature of 230°C. No print cooling was applied. The layer thickness was set to 0.15 mm, with a print speed of 25 mm/s and a fill density of 100%.

Debinding followed the Badische Anilin-und Soda-Fabrik (BASF) process, using a Nabertherm NRA 40/02-CDB debinding furnace at 120°C with HNO_3 at a concentration of >98%. Nitric acid was fed at a typical rate of 30 L/h, along with nitrogen purging gas at 500 L/h, ensuring safe and consistent processing. The debinding phase concludes upon reaching a minimal mass loss of 10.5%.

The final stage, sintering, was conducted in a 100% pure, dry hydrogen atmosphere. The sintering cycle involved a controlled temperature ramp as follows:

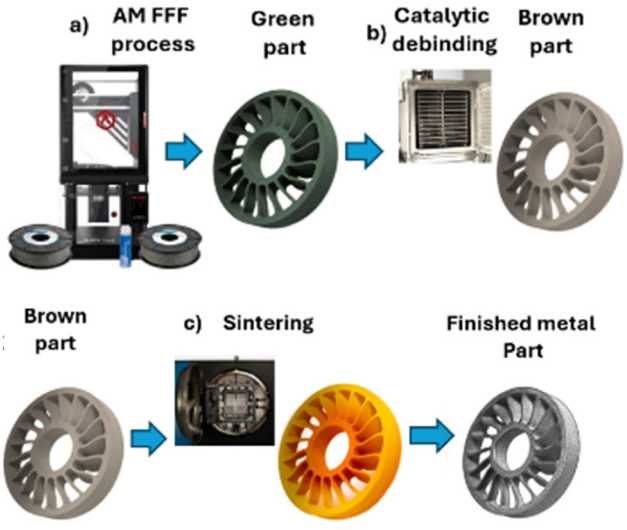

Figure 1: Ultrafuse 316L filament, created by BASF for producing stainless steel parts through 3D printing, was employed (as an example of the possibilities of FFF technology).

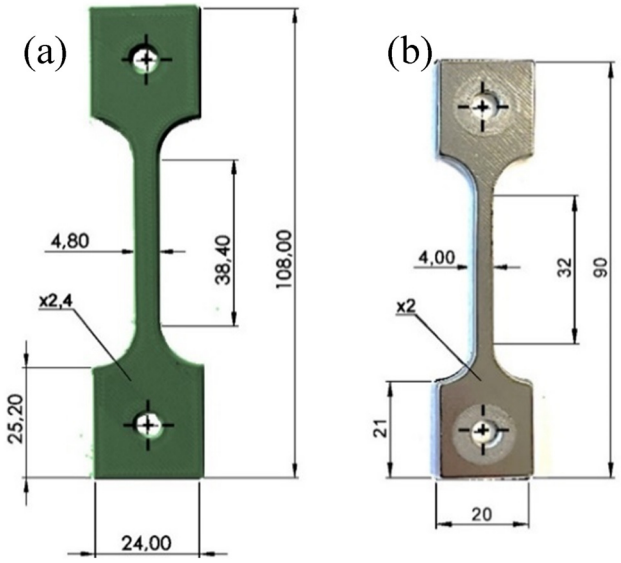

Figure 2: AM 316L specimen: (a) printed part and (b) final part after sintering.

- From room temperature to 600°C at a rate of 5 K/min, followed by a 1 h hold at 600°C.
- From 600 to 1,380°C at a rate of 5 K/min, followed by a 3 h hold at 1,380°C.
- Gradual furnace cooling to complete the process.

The initial microstructure (Figure 3) of the as-received materials in all cases consists of equiaxial grains with recrystallization twins present in some of the larger grains. The average grain size in the conventional 316L steels, equaling 19.2 µm, while FFF 316L has average grain diameter of 37 µm. All steels have a heterogeneous distribution of grain sizes.

Each specimen was divided into 14 areas, 10 of which were in the gauge section (Figure 4). In each area, the ferrite content and electromagnetic parameters were measured.

The following tests were conducted to measure the ferrite content formed during the plastic deformation of specimens:

- Manual measurement of the ferromagnetic martensitic phase content, using a DMP30 ferritoscope.
- Manual measurement of impedance parameters (phase angle and amplitude) using the lift off technique and NORTEC 600 eddy current flaw detector.
- Automatic measurement of the amplitude and resonance frequency of the eddy current signal using developed setup based on the WIROTEST device made by WIT Łukasiewicz (Figure 5).
- Profile of the ferrite phase content using XRD and XRDynamic 500 diffractometer.

Ferrite phase content, phase angle, amplitude, and resonance frequency were measured in all specimens

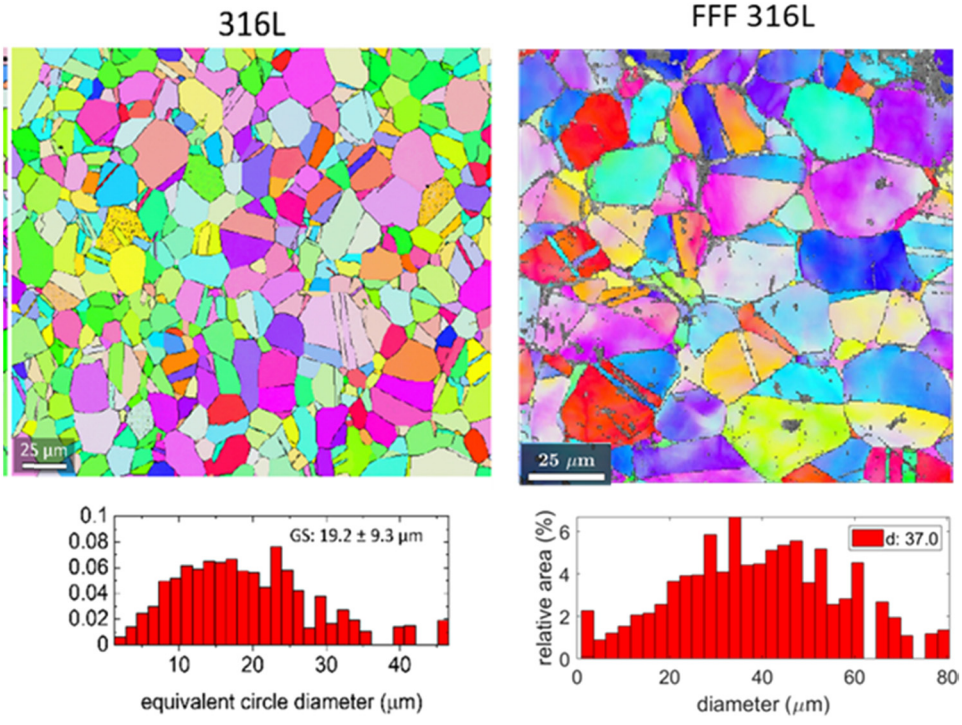

Figure 3: As-received microstructures of the investigated materials: inverse pole figure maps in the top row and grain size distributions (equivalent circle diameter) in the bottom row.

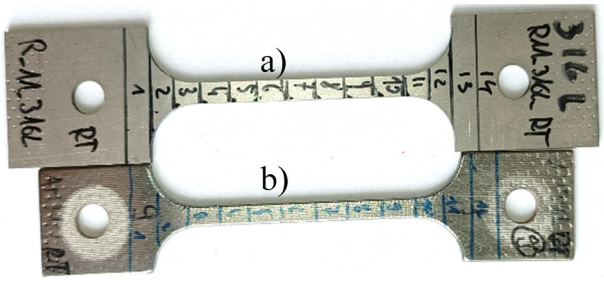

Figure 4: Specimen cut from sheet metal R 316L (a) and printed AM 316L (b).

using the above-mentioned techniques before and after static tensile tests performed up to 8% in plastic deformation. Subsequently, one series of specimens was subjected to five loading–unloading tensile cycles, to obtain 1% deformation in the first cycle, 2% in the second, 4% in the third, 6% in fourth, and 8% of plastic deformation in the last, fifth cycle. After subsequent loading cycles, the ferrite content and impedance parameters were measured in each measuring area. Measurements with the WIROTEST setup (Figure 5) and XRD tests were performed after loading. The results obtained with these techniques refer only to the state before and after plastic deformation to a certain level.

The feritscope, widely used due to its speed and non-destructive nature, provides reliable results when calibrated appropriately [23]. The feritscope measures ferromagnetic microstructures in materials, primarily ferrite but also α' martensite, which has a ferromagnetic BCC structure. It cannot measure ε martensite, as this paramagnetic, HCP phase does not generate a detectable magnetic signal. ε martensite is transitional, reducing with plastic strain and converting to α' martensite at higher strains [23,24].

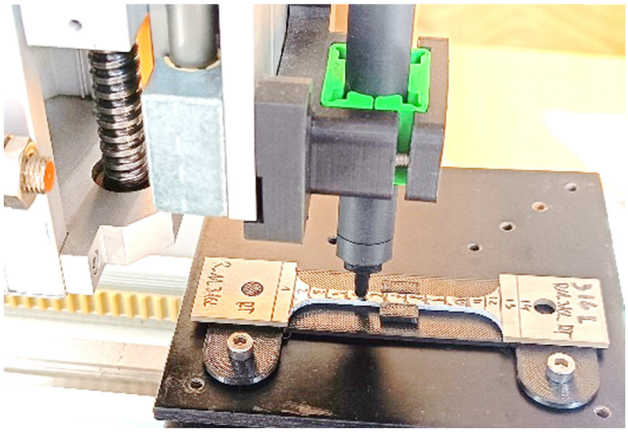

Figure 5: Automated system for measuring the amplitude and frequency of the eddy current signal by WIROTEST.

The feritscope detects voltage proportional to magnetic properties, but differences between ferrite and martensite magnetic permeability necessitate conversion of the readings. Talonen *et al.* [23] established a widely cited proportionality coefficient of 1.7 for martensite content, supported by other researchers [24].

Talonen *et al.* [23] demonstrated a linear relationship between martensite content and feritscope readings up to 55%, with a bilinear approximation beyond this. The formula for martensite content (%) based on feritscope readings is

$$M(\%) = \begin{cases} 1.7 \cdot \mathrm{Fr}, & \mathrm{Fr} \le 50 \\ 0.5357 \cdot \mathrm{Fr} + 58.2143, & \mathrm{Fr} \in \langle 50{,}78 \rangle. \end{cases}$$

The martensite content was measured using the feritscope Fisher FMP 30, an instrument that detects all magnetic phases, including ferrite. The martensite content for ASS can be calculated from the feritscope reading according to the formula presented by Talonen *et al.*

Thus, in the manuscript the ferrite content measured by means of commercial NORTEC 600 flaw detector was verified by feritoscope and WIROTEST measurement, as well as by XRD analysis.

3 Results

At the beginning of experimental procedure, three specimens of 316L steel (produced *via* rolling – R and AM) were subjected to static tensile loading at 77 K, inducing a similar plastic strain in AM and R. For these specimens, the results are reported for the states before and after deformation

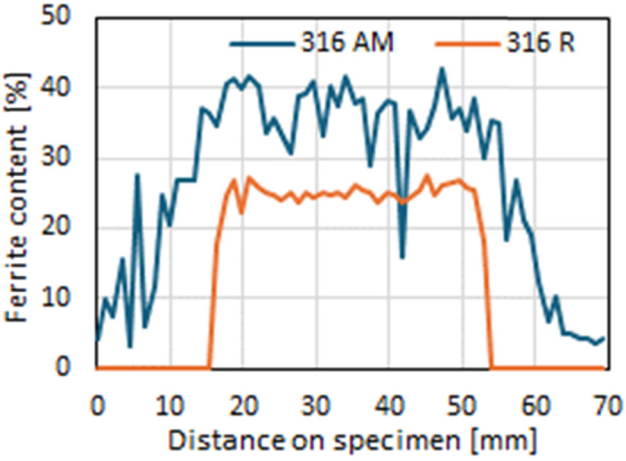

Figure 6: Profiles of ferrite content measured along the symmetry axis for the rolled (R) and printed (AM) specimens after plastic deformation at 77 K, obtained by XRD method.

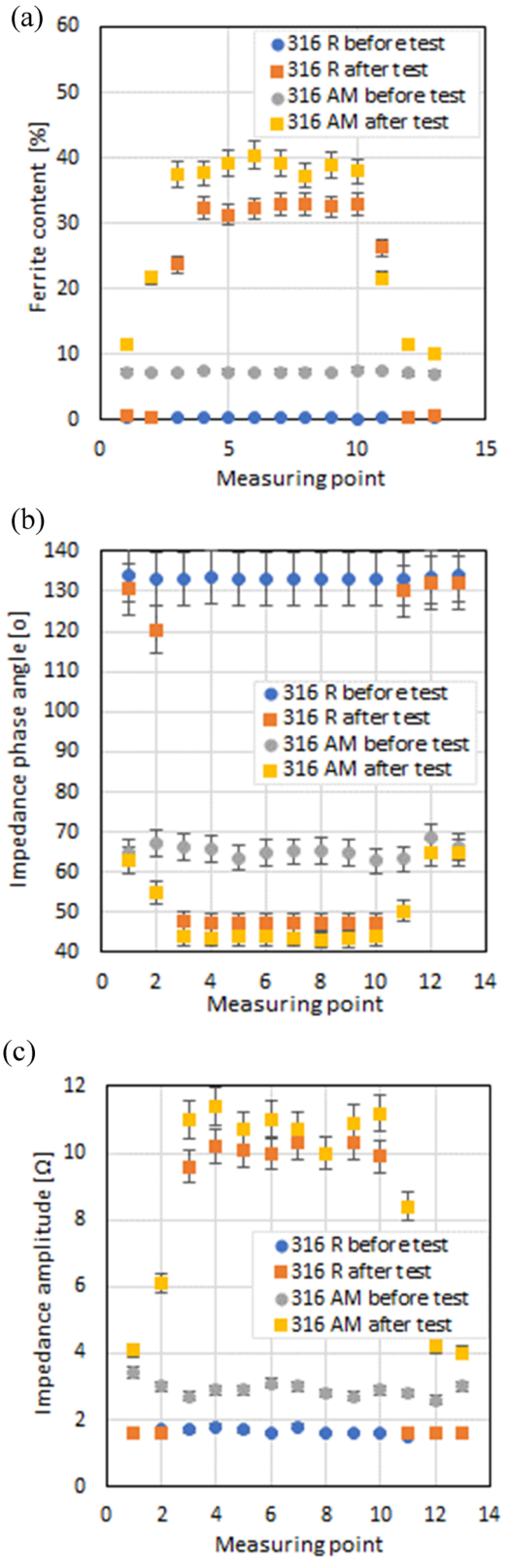

Figure 7: Profiles of ferrite content (a), phase angle (b), and impedance amplitude (c) changes measured for the rolled (R) and printed (AM) specimens, before and after deformation at 77 K.

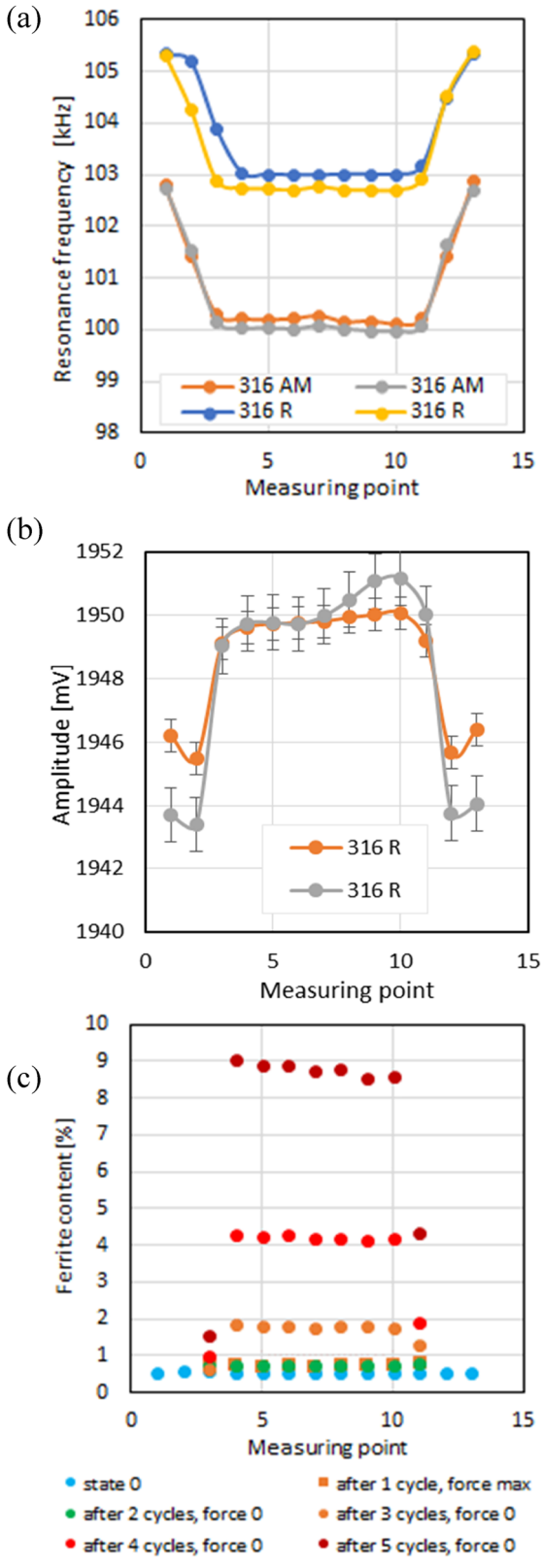

Figure 8: Resonance frequency (a) and eddy current voltage amplitude (b) obtained by WIROTEST in the scanning mode. Ferrite content profiles for five states of plastic deformation, without elastic stresses (measurement at force 0) (c).

(Figures 7 and 8). For one pair of samples (AM and R), ferrite content measurements and commercial flaw detection data were collected after each cycle of tensile loading (Figures 9 and 10). In the case of AM 316L some initial ferrite grains are present at austenite grain boundaries as a result of high temperature sintering process, while the R316L sample presents typical single-phase microstructure (Figure 3).

Figure 6 presents the ferrite phase content measured using the XRD method for two specimens manufactured by different techniques. The graphs illustrate the profile of ferrite content percentages at successive measurement points along the sample axis. To achieve a substantial amount of ferrite, experiments were carried out at 77 K (liquid nitrogen temperature). At this temperature, the deformation-induced phase transformation in austenitic steels occurs with much greater intensity compared to similar deformation conducted at room temperature [21]. This allowed for a comparison of ferrite distribution between conventionally manufactured and additively manufactured 316L steel. One can observe increased ferrite phase content in the AM specimen, both in the non-plastically deformed area (grip part) and along the entire length of the gauge area (Figure 6).

The result shown in Figure 8a shows the ferrite contents in previously specified areas of the specimens measured by using ferritoscope. Uniaxial tensile tests were carried out at 77 K. Similar to the XRD measurements, an increased ferrite phase content was observed in the printed specimens, both, in the initial state and after deformation. The similar trend was observed during phase angle measurements (Figure 7b) and impedance amplitude measurements (Figure 7c) executed by applying an eddy current probe at the established measurement points. These are the results of the sintering process of AM specimens (Figure 2).

Subsequently, measurements of the resonance frequency and the voltage amplitude of the eddy current signal induced by the WIROTEST setup developed by the authors were presented. Figure 8a shows the frequency values obtained in automatic mode for two rolled and two AM specimens after plastic deformation. Since the WIROTEST setup also measures the voltage amplitude of the induced eddy currents, Figure 9b presents the results of these measurements for two pairs of specimens after plastic deformation. The eddy current amplitude changes along the axis of plastically deformed specimens indicating the possibility of detecting deformed areas and related sensitivity to the manufacturing method and the corresponded ferrite content. Furthermore, in the case of 316R, a local increase of the amplitude value was observed. Plastic front propagation is observed in 316L, but only at 77 K. This peak is related to the presence of the martensitic transformation front [22]. The results obtained for five static load cycles

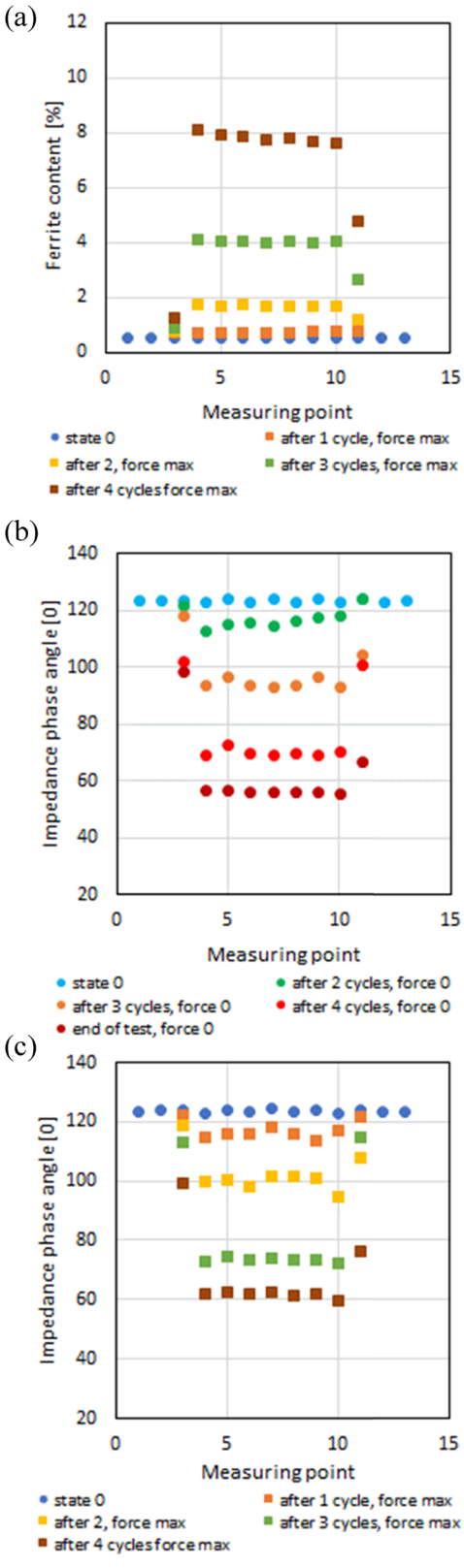

Figure 9: Ferrite content profiles (a) and eddy current phase angle profiles for five states of plastic deformation measured during unloading (b) and loading (c).

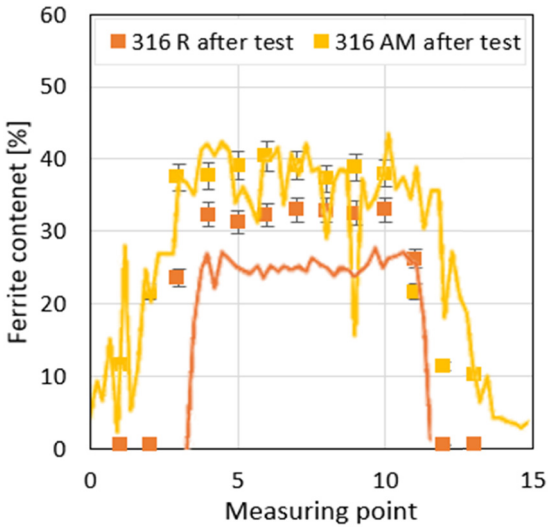

Figure 10: Comparison of ferrite content profiles for two types of SS316L after deformation obtained by XRD (line) and feritoscope (points).

are presented only for the rolled 316L steel specimen. They include measurements of the ferrite content and the phase angle value after each cycle, in the unloaded stage (force 0) and at the maximum load applied (force max). The aim of such interrupted test was to assess the effect of elastic deformation on the measurable parameters. Figure 8c shows the increase in ferrite content along the specimen axis in subsequent cycles, *i.e.*, as a function of increasing strain, for the unloaded variant. Figure 9a presents the changes in ferrite content measured at the maximum force of subsequent load cycles. With the increase of the plastic deformation level, differences in ferrite content are visible for the unloaded and maximum load conditions (Figure 9b and c). It is so called Villari effect [25,26].

4 Discussion

All applied research techniques demonstrate sensitivity to changes in the content of ferrite which result from manufacturing processes and deformation-induced phase transformation. The results of tests conducted under cyclic loading indicate the potential for identifying elastic deformation in both phases: austenite as well as in ferrite (Figures 8 and 9). This implies that flaw detector measurements, commonly used for detecting potential cracks, can also be utilized to identify and monitor the evolution of deformation-induced phase transformations in austenitic stainless steels. In the case of impedance amplitude measurements using the WIROTEST setup, two specimens exhibited a peak value near the end of the measurement section (points 10 and 11). This is likely associated with the location of the martensitic transformation front. However, this effect was not consistently observed. The results obtained from techniques based on magnetic induction demonstrate sensitivity to changes in magnetic permeability, which are linked to the presence of the ferromagnetic martensitic phase.

One should highlight the suitability of eddy current (EC) methodology in ferrite content identification. The comparison between feritscope and XRD techniques presented in Figure 10 proved the high efficiency of presented methodology.

5 Conclusions

Eddy current methodology is a promising non-destructive technique for indirectly measuring martensite formation in 316L during plastic deformation, though it comes with certain limitations. 316L, an austenitic stainless steel, can undergo deformation-induced phase transformation from austenite to martensite during, which it alters its magnetic properties. Since eddy currents are sensitive to changes in the material's electrical conductivity and magnetic permeability, they can indirectly detect the presence of martensite, which is ferromagnetic, unlike the non-magnetic austenitic phase. This makes EC a suitable method for tracking martensitic transformation in real-time during mechanical loading without interfering with the deformation process. The high sensitivity of EC to local changes in phase composition is an advantage, allowing the detection of even small volume fraction of martensite. Additionally, EC is fast, scalable, and can be applied to complex geometries, making it versatile for *in situ* industrial applications. However, its sensitivity to other factors, such as temperature variations, strain-induced microstructural changes unrelated to martensite formation, and surface condition, may complicate accurate phase quantification. Calibration with complementary techniques like XRD or magnetic Barkhausen noise analysis might be required to enhance the accuracy of martensite content determination. Thus, while EC is suitable for detecting trends in martensitic transformation during plastic deformation, precise quantification and isolation of martensite may necessitate careful control of experimental conditions and the integration of additional methodologies.

Acknowledgments: Thanks to Mirosław Wyszkowski, Andrzej Chojnacki for help with low-temperature strength tests.

Funding information: This work has been supported by the National Science Centre through Grant No UMO-2023/51/D/ST8/02370 and Polish National Agency for Academic

Exchange through Grant No BPN/BDE/2023/1/00022/U/00001/ZU/00001. The research used devices developed as part of the project entitled "Development of technology for high-pressure gas hardening of satellite gears of the epicyclic aircraft gearbox of the FDGS engine, made of Pyrowear 53 steel and operating under long-term and cyclically variable operating loads" financed under the TECHMASTRATEG II competition by the National Centre for Research and Development (No.: TECHMATSTRATEG2/406725/1/NCBR/2020).

Author contributions: All authors have accepted responsibility for the entire content of this manuscript and consented to its submission to the journal, reviewed all the results and approved the final version of the manuscript. D.K.: development of the research concept, performance of phase angle measurements, preparation of the manuscript; A.K.: measurements in the frequency range and signal amplitude; P.L.: performance of diffractometric tests and development of results; J.T.: development of the cryo-testing device and measurements of ferrite content: D.S.: EBSD tests; R.R., J.K.: preparation of specimen; A.Z.: development of the strength testing program; M.K.: development of research results and text editing.

Conflict of interest: Authors state no conflict of interest.

Data availability statement: The datasets generated during the current study are available from the corresponding author on reasonable request.

References

[1] Tavares SSM, Gunderov D, Stolyarov V, Neto JM. Phase transformation induced by severe plastic deformation in the AISI 304L stainless steel. Mater Sci Eng A. Oct 2003;358(1–2):32–6. doi: 10.1016/S0921-5093(03)00263-6.

[2] Datta K, Delhez R, Bronsveld PM, Beyer J, Geijselaers HJM, Post J. A low-temperature study to examine the role of ε-martensite during strain-induced transformations in metastable austenitic stainless steels. Acta Mater. Jun 2009;57(11):3321–6. doi: 10.1016/j.actamat.2009, 10.1016/S0925-8388(00)00874-4.

[3] Ferreri NC, Pokharel R, Livescu V, Brown DW, Knezevic M. Effects of heat treatment and build orientation on the evolution of ϵ and α' martensite and strength during compressive loading of additively manufactured 304L stainless steel. Acta Mater. 2020;195:59–70. ISSN 1359-6454, doi: 10.1016/j.actamat.2020.04.036.

[4] Tavares SSM, Fruchart D, Miraglia S. Magnetic study of the reversion of martensite α' in a 304 stainless steel. J Alloy Compd. Jul 2000;307(1–2):311–7.

[5] Bruschi S, Simonetto E, Pigato M, Ghiotti A, Bertolini R. Analysis of the AISI 316 stainless steel sheet response to sub-zero deformation temperatures. Manuf Lett. Aug 2023;35:208–14. doi: 10.1016/j.mfglet.2023.08.023.

[6] Gundgire T, Jokiaho T, Santa-aho S, Rautio T, Järvenpää A, Vippola M. Comparative study of additively manufactured and reference 316 L stainless steel samples – effect of severe shot peening on microstructure and residual stresses. Mater Charact. Sep 2022;191:112162. doi: 10.1016/j.matchar.2022.112162.

[7] Liu H, Wei Y, Tan CKI, Ardi DT, Tan DCC, Lee CJJ. XRD and EBSD studies of severe shot peening induced martensite transformation and grain refinements in austenitic stainless steel. Mater Charact. Oct 2020;168:110574. doi: 10.1016/j.matchar.2020.110574.

[8] Li Y, Luo Y, Li J, Song D, Xu B, Chen X. Ferrite formation and its effect on deformation mechanism of wire arc additive manufactured 308 L stainless steel. J Nucl Mater. Jul 2021;550:152933. doi: 10.1016/j.jnucmat.2021.152933.

[9] Zhong Y, Rännar LE, Liu L, Koptyug A, Wikman S, Olsen J, et al. Additive manufacturing of 316L stainless steel by electron beam melting for nuclear fusion applications. J Nucl Mater. Apr 2017;486:234–45. doi: 10.1016/j.jnucmat.2016.12.042.

[10] Gauss C, Souza Filho IR, Sandim MJR, Suzuki PA, Ramirez AJ, Sandim HRZ. In situ synchrotron X-ray evaluation of strain-induced martensite in AISI 201 austenitic stainless steel during tensile testing. Mater Sci Eng A. Jan 2016;651:507–16. doi: 10.1016/j.msea.2015.10.110.

[11] Haušild P, Davydov V, Drahokoupil J, Landa M, Pilvin P. Characterization of strain-induced martensitic transformation in a metastable austenitic stainless steel. Mater Des. Apr 2010;31(4):1821–7. doi: 10.1016/j.matdes.2009.11.008.

[12] Li J, Fang C, Liu Y, Huang Z, Wang S, Mao Q, et al. Deformation mechanisms of 304L stainless steel with heterogeneous lamella structure. Mater Sci Eng A. Jan 2019;742:409–13. doi: 10.1016/j.msea.2018.11.047.

[13] Lois A, Ruch M. Assessment of martensite content in austenitic stainless steel specimens by eddy current testing. Insight Non Destr Test Cond Monit. 2006;48:26–9.

[14] Sohrabi MJ, Naghizadeh M, Mirzadeh H. Deformation-induced martensite in austenitic stainless steels: a review. Arch Civ Mech Eng. 2020;20:124. doi: 10.1007/s43452-020-00130-1.

[15] Solomon N, Solomon I. Effect of deformation-induced phase transformation on AISI 316 stainless steel corrosion resistance. Eng Failure Anal. 2017;79:865–75. Elsevier Ltd, doi: 10.1016/j.engfailanal.2017.05.031.

[16] Solomon N, Solomon I. Deformation induced martensite in AISI 316 stainless steel. Rev Met. Mar 2010;46(2):121–8. doi: 10.3989/revmetalm.0920.

[17] Takaki S, Fukunaga K, Syarif J, Tsuchiyama T. Effect of grain refinement on thermal stability of metastable austenitic steel. Mater Trans. 2004;45(7):2245–51. doi: 10.2320/matertrans.45.2245.

[18] Stalder M, Vogel S, Bourke MAM, Maldonado JG, Thoma DJ, Yuan VW. Retransformation ($\alpha' \rightarrow \gamma$) kinetics of strain induced martensite in 304 stainless steel. Mater Sci Eng A. 2000;280:270–81.

[19] Normando PG, Moura EP, Souza JA, Tavares SSM, Padovese LR. Ultrasound, eddy current and magnetic Barkhausen noise as tools for sigma phase detection on a UNS S31803 duplex stainless steel. Mater Sci Eng A. May 2010;527(12):2886–91. doi: 10.1016/j.msea.2010.01.017.

[20] Nalepka K, Skoczeń B, Ciepielowska M, Schmidt R, Tabin J, Schmidt E, et al. Phase transformation in 316l austenitic steel induced by fracture at cryogenic temperatures: experiment and modelling. Materials. 2021;14:127.

[21] Spencer K, Véron M, Yu-Zhang K, Embury JD. The strain induced martensite transformation in austenitic stainless steels: Part 1 – influence of temperature and strain history. Mater Sci Technol. 2009;25:7–17.
[22] Tabin J, Nalepka J, Kawałko K, Brodecki A, Bała P, Kowalewski Z. Plastic flow instability in 304 austenitic stainless steels at room temperature. Metall Mater Trans A. 2023;54:4606–11.
[23] Talonen J, Aspegren P, Hänninen H. Comparison of different methods for measuring strain induced α-martensite content in austenitic steels. Mater Sci Technol. 2004;20:1506–12.
[24] Somani MC, Juntunen P, Karjalainen LP, Misra RDK, Kyröläinen A. Enhanced mechanical properties through reversion in metastable austenitic stainless steels. Metall Mater Trans A. 2009;40:729–44.
[25] Glage A, Weidner A, Biermann H. Effect of austenite stability on the low cycle fatigue behavior and microstructure of high alloyed metastable austenitic cast TRIP steels. Procedia Eng. 2010;2:2085–94.
[26] Domenjoud M, Daniel L. Effects of plastic strain and reloading stress on the magneto-mechanical behavior of electrical steels: experiments and modeling. Mech Mater. 2023;176:104510. doi: 10.1016/j.mechmat.2022.104510.